



Designing a sliding mode controller for a class of multi-controller COVID-19 disease model

M. Gholami, S.M. Mirhosseini-Alizamini*,^{} and A. Heidari^{}

Abstract

The recent outbreak of the COVID-19 disease has just appeared at the end of 2019 that has now become a global pandemic. Analysis of mathematical models in the prediction and control of this pandemic helps to make the right decisions about vaccination, quarantine, and other control measures. In this article, the aim is to analyze the three control measures of educational campaigns, social distancing, and treatment control, that these

*Corresponding author

Received ??? ; revised ??? ; accepted ???

Morteza Gholami

Department of Mathematics, Payame Noor University (PNU), P.O. Box 19395-4697, Tehran, Iran. e-mail: Morteza.gholami63@gmail.com

Seyed Mehdi Mirhosseini-Alizamini

Department of Mathematics, Payame Noor University (PNU), P.O. Box 19395-4697, Tehran, Iran. e-mail: m_mirhosseini@pnu.ac.ir

Aghileh Heydari

Department of Mathematics, Payame Noor University (PNU), P.O. Box 19395-4697, Tehran, Iran. e-mail: a_heidari@pnu.ac.ir

How to cite this article

Gholami, M., Mirhosseini-Alizamini, S.M. and Heydari, A., Designing a sliding mode controller for a class of multi-controller COVID-19 disease model. *Iran. J. Numer. Anal. Optim.*, ??; ??(??): ??-??. ??

control measures can reduce the spread of this disease. For this purpose, due to the uncertainty in the model parameters, a sliding mode control law is used. Furthermore, because the model parameters are changing and the upper limit of the parameters that have uncertainty should be known, then an adaptive control is used to estimate the switching gain online. In addition, in order to prevent the chattering phenomenon, the sign function is used in the sliding control law. Also, the obtained properties are expressed and proven analytically. Therefore, initially, the controller is designed assuming certain knowledge of an upper bound of the uncertainty signal. After that, the parameters that have uncertainty in the simulation are obtained by online estimation of the adaptive control. The efficiency and performance of the controller in the absence of the certainty of the model parameters are investigated, and the results show the desired performance of this controller. Finally, the performance and efficiency of the controller are evaluated by simulation.

AMS subject classifications (2020): 93C10, 49N10, 93C43.

Keywords: COVID-19; Sliding mode control; Uncertainty; Mathematical model; Social distancing.

1 Introduction

Infectious diseases, whether in the past, such as cholera, plague, and so on, or currently, the COVID-19, have challenged human societies and have always been one of the main causes of death even in developed countries. Since it is always possible for a new infection to appear or previous infections to re-emerge and increase, it is very important to study these diseases in order to predict, control, and treat them. It also poses a huge risk to public health and economics all over the world [12, 48]. In the meantime, mathematical models have been used to analyze the performance of this disease in recent research to deal with and eliminate the disease [13, 21, 36]. A review of these studies and similar studies shows that differential equations are often used in most models and they solve and investigate the problem by simplifying it [15, 42]. In [18, 19], the simplest type of epidemic modeling includes susceptible, infected, and recovered (SIR) people for this disease. Also, a simple model

is considered in [40], but this model cannot show all the behaviors of this disease. Due to the different nature of this virus, it is felt necessary to add new groups for a more accurate study of the disease. Das and Samanta [20] studied a mathematical model for investigating the COVID-19 disease in Japan, in which the group of infected people is divided into two categories: “infection without symptoms and infection with symptoms”(SAIR). Also, in [9, 17, 45, 46, 49], a simple model of the COVID-19 disease has been investigated in order to take measures to prevent the spread of this disease. In [45, 46], other parts were added to these simple models (SIR) in order to have a better examine for this disease.

Some other models try to investigate this process by using statistics and probability tools. Indeed unfortunately, these models are usually not able to describe many details and examine them correctly due to simplifications [47], Authors collected individual-case data for patients who died from COVID-19 in Hubei, mainland China and for cases outside of mainland China. These individual-case data were used to estimate the time between onset of symptoms and outcome (death or discharge from hospital). There are also many other mathematical models that reported on COVID-19 pandemics; see [22, 32]. In [39] mathematical models developed were mainly used to investigate the effects of different non-pharmaceutical intervention strategies via simulation using different computing soft-wares.

However, with regard to the spread and infectivity of the disease, one of the important features of the model is stability, which indicates whether the disease persists or disappears [31, 41, 54]. One of the most fundamental issues when studying stability is the determination of the so-called reproduction number of the model, R_0 . Mukandavire et al. [35] quantified the COVID-19 outbreak in South Africa, explored the efficacy of vaccine scenarios, and obtained a basic reproduction number of 2.94. Finally, studies have shown that current social distancing measures to reduce contact have been successful in controlling infection in the absence of a vaccine and other key treatments.

With the introduced control, such as quarantine, the basic reproduction number R_0 decreased from 1.83 to 1.23 for India [8, 43], which shows that India has been able to control the disease to some extent. Studied the impact of non-pharmaceutical interventions in curtailing the 2019 novel Coronavirus in

the US state of New York and the entire US. The research demonstrated that using face-masks in public is very useful in minimizing community transmission and burden of COVID-19, provided their coverage level is high [37].

The prolongation of the pandemic will not only increase the death rate of the population but also increase the medical and health costs to prevent the spread and eliminate the virus in the society and will cause economic losses. So when the epidemic trend of infectious disease arises, compulsory treatment is an efficient pattern to control the rapid spreading. So in [52], a sliding mode is carried out to evaluate the effect of compulsory treatment in infectious disease controlling when the number of infected persons reaches a certain level, the policy of compulsory treatment will be carried out at certain rate.

Sliding mode control (SMC) is a powerful approach to control non-linear and non-deterministic systems. Sliding control is a robust control method and can be used with uncertainties and parameter disturbances, provided that the range of these uncertainties and disturbances is known. Therefore, SMC is considered a very suitable method for controlling non-linear systems with uncertainty of parameters.

SMC has been widely developed, such as higher order SMC [7, 30] and dynamic SMC [28, 51]. Meanwhile, SMC is one of the most well-known and widespread methods due to its simple design process and suitable results. Therefore, this controller has been successfully applied to robotics, vehicle dynamics [50, 53], chemical engineering [16, 29, 26], and electrical systems [3, 4].

One of the SMC approaches is the linear quadratic regulator method [33, 34], which is also an original method. Of course, in recent years, the optimization and approximation of some systems that have a time delay have also been considered [1, 24, 25, 27]. Some applications of SMC are described in [55, 23]. It has explained about the selection of the appropriate sliding surface [2]. One of the important advantages of SMC is its invariance to uncertainties. Because of this advantage, SMC is a powerful tool dealing with structural or unstructured disturbances, disturbance, and noise. The most important drawback of SMC is chattering. Chattering is high frequency (but limited) fluctuations with low amplitude, which causes thermal losses in power circuits

and wear of mechanical parts [44]. Chattering is caused by the stimulation and oscillation of unmodeled or unknown high frequency dynamics of sensors, actuators, or the system itself [5, 6, 38]. One of the methods to reduce or eliminate chattering is the use of adaptive control that although chattering is not completely eliminated in this method, but it is reduced. This chattering causes problems, and sometimes, it can make system performance unstable. The system considered here also has uncertainty, so that the adaptive control can update the system parameters [14]. Thus, in order to avoid the chattering phenomenon, switching gain adaptation is used here. In this work, for this adaptation, the value of the gain in the simulation is considered zero first, and its value increases until the slip condition is established; that is, the estimation is done online.

In this paper, a mathematical model for COVID-19 relevant to study the transmission dynamics of coronavirus in Bangladesh [11] is developed, and this paper presents the design an adaptive sliding mode controller for the epidemic model. This designed control law is able to protect the entire total population time regardless of the uncertainty of the model parameters. Usually, the SMC needs to consider the information of the bounds of the uncertainties. This assumption may also seem somewhat unrealistic in epidemic models because the exact value of the parameters is not known. Therefore, the designed SMC for epidemic then improves the sliding gain value with an adaptive control. Finally, the numerical results show that the whole system guarantees the eradication of epidemics. Also, the mathematical proof of all the stated results, including the positivity of the solutions, the boundedness of the solutions, the existence of the solutions, and the stability of the sliding mode controllers, have been developed in this article.

The rest of this paper is as follows: In Section 2, the statement of the desired problem is explained, along with the introduction of the system model. In Section 3, a suitable sliding surface of integral type is defined, and the adaptive SMC is applied to the model with parameter uncertainty. Then, in order to investigate the performance of the controller, numerical simulation in Section 4 is done. Finally, in Section 5, we give concluding remarks and future directions for further studies.

2 The mathematical model

The model that is studied and analyzed in this article, model $SQIIsR$, is derived from the model of [11], considering that quarantine and isolation of people are important things to prevent and spread the disease, so it has been obtained by adding parts to the simple model SIR . This mathematical model for COVID-19 is developed in [11] and in which the total population is divided into five groups:

- $S(t)$; Susceptible, people who are not affected by the coronavirus infections but any time they may be infected.
- $Q(t)$; Quarantined, people who are in contact with susceptible people and have high possibility of carrying the infection.
- $I(t)$; Infected, people who are infected by the disease and show some symptoms they can transmit the infections any time.
- $I_s(t)$; Isolated, people who are identified with coronavirus infections and they are isolated to a separate place for treatment.
- $R(t)$; Recovered, people who are have recovered and thus have the immunity or have died from the disease and thus cannot contribute to further disease transmission.

Let $N(t)$ be the total population at time t , that is:

$$N(t) = S(t) + Q(t) + I(t) + R(t) + I_s(t). \quad (1)$$

The state space equations of this model are as follows:

$$\begin{cases} \frac{dS(t)}{dt} = \kappa - (\alpha Q(t) + \varphi I(t))S(t) - \beta_0 S(t) + \varepsilon R(t) - u_1 S(t), \\ \frac{dQ(t)}{dt} = \alpha Q(t)S(t) - \beta_0 Q(t) - \beta Q(t) - \lambda Q(t), \\ \frac{dI(t)}{dt} = \beta Q(t) + \varphi I(t)S(t) - (\theta + \delta + \beta_0)I(t) - u_2 I(t), \\ \frac{dI_s(t)}{dt} = \delta I(t) - \sigma I_s(t) - \beta_0 I_s(t) - \mu I_s - (u_2 + u_3)I_s(t), \\ \frac{dR(t)}{dt} = \delta I_s(t) - \beta_0 R(t) + \theta I(t) + \lambda Q(t) - \varepsilon R(t) + u_1 S(t) + u_2 I(t) + (u_2 + u_3)I_s(t), \end{cases} \quad (2)$$

where $S(0) \geq 0$, $Q(0) \geq 0$, $I(0) \geq 0$, $I_s(0) \geq 0$, and $R(0) \geq 0$ are the initial state. Also, all parameters have uncertainty and have a value between zero and one.

Because there is no definitive treatment or vaccine for this virus, the following strategies are suggested: there are three controls $u_1(t)$, $u_2(t)$, and $u_3(t)$ for all $t \in [0, T]$:

- $u_1(t)$; educational campaign, the first control, can be interpreted as the proportion to be subjected to sensitization and prevention. So, we note that u_1 is the awareness program for susceptible people at time t .
- $u_2(t)$; social distancing, the second control, maintenance of social distancing, which has been considered only effective step ever now to control the transmission of this disease. This control represents preventive actions like quarantine isolation and lockdowns which lower the contact rate between different groups of people in a society. Therefore, this control can be interpreted as a quarantine to reduce the transmission of this health virus.
- $u_3(t)$; treatment control, the last control $u_3(t)$ treatment of the patients on the basis of the symptoms to minimize their sufferings and serious medical care that helps infected individuals to recover from the disease as fast as possible.

Also, the first control is related to before infection, and the other two controls are related to after infection. The following theorem is used to check whether the states (number of people) are always positive in the stated model.

Theorem 1. If $S(0) \geq 0$, $Q(0) \geq 0$, $I(0) \geq 0$, $I_s(0) \geq 0$, and $R(0) \geq 0$, then solutions $S(t)$, $Q(t)$, $I(t)$, $I_s(t)$, and $R(t)$ in system (2) for $t \geq 0$ are always positive.

Proof. From the first equation of system (2) according to the initial conditions, it follows that

$$\begin{aligned} \frac{dS(t)}{dt} &= \kappa - \left(\alpha Q(t) + \varphi I(t) \right) S(t) - \beta_0 S(t) + \varepsilon R(t) \\ &\geq - \left(\alpha Q(t) + \varphi I(t) \right) S(t) - \beta_0 S(t). \end{aligned} \quad (3)$$

Then

$$\frac{dS(t)}{dt} + \left(\alpha Q(t) + \varphi I(t) + \beta_0 \right) S(t) \geq 0. \quad (4)$$

Let

$$G(t) = \alpha Q(t) + \varphi I(t) + \beta_0. \quad (5)$$

If the both sides in inequality (4) are multiplied by $\exp\left(\int_0^t G(s)ds\right)$, then we obtain

$$\exp\left(\int_0^t G(s)ds\right) \cdot \frac{dS(t)}{dt} + G(t) \cdot \exp\left(\int_0^t G(s)ds\right) \cdot S(t) \geq 0. \quad (6)$$

Thus

$$\frac{d}{dt} \left(S(t) \cdot \exp\left(\int_0^t G(s)ds\right) \right) \geq 0. \quad (7)$$

Integrating this inequality (7) from 0 to t gives

$$\int_0^t \frac{d}{ds} \left(S(s) \cdot \exp\left(\int_0^s (\alpha Q(s) + \varphi I(s) + \beta_0)ds\right) \right) ds \geq 0. \quad (8)$$

Then

$$S(t) \geq S(0) \cdot \exp\left(-\int_0^t (\alpha Q(t) + \varphi I(t) + \beta_0)ds\right) \geq 0. \quad (9)$$

As a result, $S(t)$ is always positive. Similarly, we prove that $Q(t) \geq 0, I(t) \geq 0, I_s \geq 0$ and $R(t) \geq 0$. That is,

$$\begin{aligned} Q(t) &\geq Q(0) \cdot \exp\left(-\int_0^t (\beta_0 + \beta + \lambda)ds\right) \geq 0, \\ I(t) &\geq I(0) \cdot \exp\left(-\int_0^t (\theta + \delta + \beta_0)ds\right) \geq 0, \\ I_s(t) &\geq I_s(0) \cdot \exp\left(-\int_0^t (\beta_0 + \mu + \sigma)ds\right) \geq 0, \\ R(t) &\geq R(0) \cdot \exp\left(-\int_0^t (\beta_0 + \varepsilon)ds\right) \geq 0. \end{aligned} \quad (10)$$

In the following theorems, boundedness and existence of the system (2) solutions of are checked. \square

Theorem 2 (Boundedness of the solutions). The set $\Omega = \left\{ (S, Q, I, I_s, R) \in \mathbb{R}_+^5; 0 \leq S + Q + I + I_s + R \leq \frac{\kappa}{\beta_0} \right\}$ is positively invariant under system (2) with initial conditions $S(0) \geq 0, Q(0) \geq 0, I(0) \geq 0, I_s(0) \geq 0$, and $R(0) \geq 0$.

Proof. Derivation from relation (1), according to system (2), gives

$$\begin{aligned}
\frac{dN(t)}{dt} &= \frac{dS(t)}{dt} + \frac{dQ(t)}{dt} + \frac{dI(t)}{dt} + \frac{dI_s(t)}{dt} + \frac{dR(t)}{dt} \\
&= \kappa - \beta_0 \underbrace{\left(S(t) + Q(t) + I(t) + I_s(t) + R(t) \right)}_{N(t)} - \mu I_s(t) \\
&= \kappa - \beta_0 N(t) - \mu I_s(t) \\
&\leq \kappa - \beta_0 N(t).
\end{aligned} \tag{11}$$

By deriving from $\exp(\beta_0 t) \cdot N(t)$ and also with (11), we have

$$\begin{aligned}
\frac{d}{dt} \exp(\beta_0 t) \cdot N(t) &= \beta_0 \exp(\beta_0 t) N(t) + \exp(\beta_0 t) \frac{dN(t)}{dt} \\
&\leq \beta_0 \exp(\beta_0 t) N(t) + \exp(\beta_0 t) (\kappa - \beta_0 N(t)) \\
&= \kappa \exp(\beta_0 t).
\end{aligned} \tag{12}$$

By integrating on both sides of inequality (12) between 0 and t and according to the initial conditions, we have

$$\exp(\beta_0 t) N(t) - N(0) \leq \frac{\kappa}{\beta_0} (\exp(\beta_0 t) - 1). \tag{13}$$

By multiplying both sides of the inequality (13) in $\exp(-\beta_0 t)$, we have

$$\begin{aligned}
N(t) &\leq N(0) \exp(-\beta_0 t) + \frac{\kappa}{\beta_0} (1 - \exp(-\beta_0 t)) \\
&\leq N(0) \exp(-\beta_0 t) + \frac{\kappa}{\beta_0}.
\end{aligned} \tag{14}$$

If we take $\lim t \rightarrow \infty$, we have $0 \leq N(t) \leq \frac{\kappa}{\beta_0}$. It implies that the region Ω is a positivity invariant set for the system (2). Therefore, all the system (2) solutions with initial conditions are bounded. So, there exist positive constants Z_1, Z_2, Z_3, Z_4 , and Z_5 such that for all $t \in [0, T]$:

$$S(t) \leq Z_1, \quad Q(t) \leq Z_2, \quad I(t) \leq Z_3, \quad I_s(t) \leq Z_4, \quad R(t) \leq Z_5.$$

□

Theorem 3 (Existence of solutions). The system (2) that satisfies a given initial condition has a unique solution.

Proof. Let

$$X = \begin{bmatrix} S(t) \\ Q(t) \\ I(t) \\ I_s(t) \\ R(t) \end{bmatrix}, \quad \Phi(X) = \begin{bmatrix} \frac{dS(t)}{dt} \\ \frac{dQ(t)}{dt} \\ \frac{dI(t)}{dt} \\ \frac{dI_s(t)}{dt} \\ \frac{dR(t)}{dt} \end{bmatrix}. \quad (15)$$

Then the system (2) can be rewritten in the following form:

$$\Phi(X) = AX + B(X), \quad (16)$$

where

$$A = \begin{bmatrix} -\beta_0 & 0 & 0 & 0 & \varepsilon \\ 0 & -(\beta_0 + \beta + \lambda) & 0 & 0 & 0 \\ 0 & \beta & -(\beta_0 + \delta + \theta) & 0 & 0 \\ 0 & 0 & \delta & -(\beta_0 + \sigma + \mu) & 0 \\ 0 & 0 & \theta & \sigma & -(\beta_0 - \lambda + \varepsilon) \end{bmatrix}, \quad (17)$$

and

$$B(X) = \begin{bmatrix} \kappa - (\alpha Q(t) + \varphi I(t))S(t) \\ \alpha Q(t)S(t) \\ \varphi I(t)S(t) \\ 0 \\ 0 \end{bmatrix}. \quad (18)$$

The second term on the right-hand side of (16) for X_1 and X_2 satisfies

$$\begin{aligned} |B(X_1) - B(X_2)| &= |(\alpha Q_1 + \varphi I_1)S_1 - (\alpha Q_2 + \varphi I_2)S_2 \\ &\quad + \alpha Q_1 S_1 - \alpha Q_2 S_2 + \varphi I_1 S_1 - \varphi I_2 S_2| \\ &= 2|\alpha(Q_1 S_1 - Q_2 S_2) + \varphi(I_1 S_1 - I_2 S_2)| \\ &= 2|\alpha Q_1 S_1 + \alpha Q_1 S_2 - \alpha Q_1 S_2 \\ &\quad - \varphi I_1 S_1 + \varphi I_1 S_2 - \varphi I_1 S_2 - \alpha Q_2 S_2 + \varphi I_2 S_2| \\ &\leq 2\left(|\alpha Q_1| |S_1 - S_2| + |\alpha S_2| |Q_1 - Q_2|\right) \end{aligned}$$

$$\begin{aligned}
& + |\varphi I_1| |S_1 - S_2| + |\varphi S_2| |I_1 - I_2| \Big) \\
& \leq 2 \frac{Z}{\beta_0} \left(|\alpha| |S_1 - S_2| + |\alpha| |Q_1 - Q_2| \right. \\
& \quad \left. + |\varphi| |S_1 - S_2| + |\varphi| |I_1 - I_2| \right) \\
& \leq M \|X_1(t) - X_2(t)\|_\infty, \tag{19}
\end{aligned}$$

Then

$$\|\Phi(X_1) - \Phi(X_2)\| \leq V \|X_1 - X_2\|, \tag{20}$$

where $V = \max(M, \|A\|) \leq \infty$. Thus, it follows that the function Φ in (16) is uniformly Lipschitz continuous, and the restriction on $S(t) \geq 0, Q(t) \geq 0, I(t) \geq 0, I_s(t) \geq 0$ and $R(t) \geq 0$. So, there is a solution for the system (2) [10]. \square

3 SMC design

This section contains the design of an SMC for the model (2) so that all the population becomes Recovered. Thus, define the tracking error as

$$e(t) = R(t) - N_d(t), \tag{21}$$

where $R(t)$ denotes the number of Recovered population at each time while $N_d(t)$ is a tracking reference signal satisfying (in order for the tracking task to be achievable with a finite control):

$$N_d(0) = R(0), \tag{22}$$

$$N_d(t) - N(t) \longrightarrow 0, \quad t \longrightarrow \infty. \tag{23}$$

Equation (22) shows that initially the tracking error in (21) is zero, that is ($e(0) = 0$), means that all the population tends to be Recovered. The proposed reference signal used in this paper is exponentially selected as

$$N_d(t) = (R(0) - N(0))e^{-at} + N(t), \tag{24}$$

where the parameter $a > 0$ controls the rate at which the reference signal converges to the total population. The sliding surface to achieve this control is defined as follows:

$$\zeta(t) = e(t) + \Gamma \int_0^t e(\tau) d\tau, \quad (25)$$

where Γ is a constant positive gain. The control law is designed in two steps. Firstly, an equivalent control U_{eq} is calculated in such a way that the sliding surface could be reached. So we obtain the derivative of the sliding surface (25):

$$\begin{aligned} \dot{\zeta}(t) &= \dot{e}(t) + \Gamma e(t) \\ &= (\dot{R}(t) - \dot{N}_d(t)) + \Gamma(R(t) - N_d(t)) \\ &= \underbrace{\sigma I_s(t) - \beta_0 R(t) + \theta I(t) + \lambda Q(t) - \varepsilon R(t) + u_1 S(t) + u_2 I(t) + (u_2 + u_3) I_s(t)}_{\dot{R}} \\ &\quad + ae^{-at}(R(0) - N(0)) - \underbrace{(\kappa - \beta_0 N(t) - \mu I_s(t))}_{\dot{N}} + \Gamma(R(t) - N(t)) \\ &\quad - \Gamma e^{-at}(R(0) - N(0)). \end{aligned} \quad (26)$$

For simplicity, take $a = \Gamma$ and then by setting the right side of equation (26) equal to zero, we get

$$\begin{aligned} \sigma I_s(t) - \beta_0 R(t) + \theta I(t) + \lambda Q(t) - \varepsilon R(t) + u_1 S(t) + u_2 I(t) + (u_2 + u_3) I_s(t) \\ - \kappa + \beta_0 N(t) + \mu I_s(t) + \Gamma R(t) - \Gamma N(t) = 0. \end{aligned} \quad (27)$$

The following equivalent controls are solutions for (27):

$$\begin{aligned} U_{1,eq} &= \frac{1}{S(t)} \left\{ \kappa + R(t)(\beta_0 + \varepsilon - \Gamma) + N(t)(\Gamma - \beta_0) - I_s(t)(\mu + \sigma) - Q(t)\lambda - \theta I(t) \right\}, \\ U_{2,eq} &= \frac{1}{I(t) + I_s(t)} \left\{ \kappa + R(t)(\beta_0 + \varepsilon - \Gamma) + N(t)(\Gamma - \beta_0) - I_s(t)(\mu + \sigma) - Q(t)\lambda - \theta I(t) \right\}, \\ U_{3,eq} &= \frac{1}{I_s(t)} \left\{ \kappa + R(t)(\beta_0 + \varepsilon - \Gamma) + N(t)(\Gamma - \beta_0) - I_s(t)(\mu + \sigma) - Q(t)\lambda - \theta I(t) \right\}. \end{aligned} \quad (28)$$

Because system (2) has uncertainty and the exact value of the parameters are not known, then

$$\begin{aligned}
\beta_0 + \epsilon - \Gamma &= \nu, & \hat{\beta}_0 + \hat{\epsilon} - \hat{\Gamma} &= \hat{\nu}, \\
\Gamma - \beta_0 &= \vartheta, & \hat{\Gamma} - \hat{\beta}_0 &= \hat{\vartheta}, \\
\mu + \sigma &= \rho, & \hat{\mu} - \hat{\sigma} &= \hat{\rho}.
\end{aligned} \tag{29}$$

So according to the nominal parameters (29) the equivalent control law (28) is as follows:

$$\begin{aligned}
U_{1,eq} &= \frac{1}{S(t)} \left\{ \hat{\kappa} + R(t)\hat{\nu} + N(t)\hat{\vartheta} - I_s(t)\hat{\rho} - Q(t)\hat{\lambda} - I(t)\hat{\theta} \right\}, \\
U_{2,eq} &= \frac{1}{I(t) + I_s(t)} \left\{ \hat{\kappa} + R(t)\hat{\nu} + N(t)\hat{\vartheta} - I_s(t)\hat{\rho} - Q(t)\hat{\lambda} - I(t)\hat{\theta} \right\}, \\
U_{3,eq} &= \frac{1}{I_s(t)} \left\{ \hat{\kappa} + R(t)\hat{\nu} + N(t)\hat{\vartheta} - I_s(t)\hat{\rho} - Q(t)\hat{\lambda} - I(t)\hat{\theta} \right\}.
\end{aligned} \tag{30}$$

The equivalent controls (30) are expressed in the following nonlinear way to avoid the chattering phenomenon:

$$\begin{aligned}
U_1 &= U_{1,eq} - \frac{K}{S(t)} \cdot \text{sgn}(\zeta(t)), \\
U_2 &= U_{2,eq} - \frac{K}{I(t) + I_s(t)} \cdot \text{sgn}(\zeta(t)), \\
U_3 &= U_{3,eq} - \frac{K}{I_s(t)} \cdot \text{sgn}(\zeta(t)),
\end{aligned} \tag{31}$$

where $\text{sgn}(x)$ is the sign function defined as

$$\text{sgn}(x) = \begin{cases} 1, & x > 0, \\ 0, & x = 0, \\ -1, & x < 0. \end{cases} \tag{32}$$

Moreover, K is a gain that must be designed so that it can overcome the parameters of system (2), which has uncertainty, and gives the desired result. Therefore, the controls law (31) allows to guaranteeing the convergence to zero of the tracking error (21) as proved in the continuation of Theorem 4. The switching gain is defined based on the following assumptions:

1. Suppose that the estimation error is f by a known bounded function F as follows:

$$|\hat{f} - f| < F, \tag{33}$$

where

$$\begin{aligned}\hat{f} &= \hat{\kappa} + R(t)\hat{\vartheta} + N(t)\hat{\nu} - I_s(t)\hat{\rho} - Q(t)\hat{\lambda} - I(t)\hat{\theta}, \\ f &= \kappa + R(t)\vartheta + N(t)\nu - I_s(t)\rho - Q(t)\lambda - I(t)\theta.\end{aligned}\quad (34)$$

This assumption shows that although the system has uncertainty parameters and there is a mismatch between these parameters, it is bounded.

2. The switching gain is selected as

$$K = F + \eta, \quad (35)$$

with $\eta > 0$ arbitrary. This assumption shows how to choose the right gain to achieve the desired results.

Theorem 4. Consider the model system (2) with the controls law (31). Thus, if Assumptions 1 and 2 hold, then the tracking error $e(t)$ vanishes asymptotically.

Proof. Consider the Lyapunov candidate function

$$L(t) = \frac{1}{2}\zeta(t)^2. \quad (36)$$

The derivative of the Lyapunov function (36) is calculated as follows:

$$\begin{aligned}\dot{L}(t) &= \zeta(t)\dot{\zeta}(t) \\ &= \zeta(t)(\dot{e}(t) + \Gamma e(t)) \\ &= \zeta(t)\left(\sigma I_s(t) - \beta_0 R(t) + \theta I(t) + \lambda Q(t) - \varepsilon R(t) + u_1 S(t) - \kappa + \beta_0 N(t) + \mu I_s(t) + \Gamma R(t) - \Gamma N(t)\right) \\ &= \zeta(t)\left(u_1 S(t) - \kappa + I_s(t)(\sigma + \mu) - R(t)(-\Gamma + \beta_0 + \varepsilon) - N(t)(-\beta_0 + \Gamma) + \lambda Q(t) + \theta I(t)\right) \\ &= \zeta(t)\left(u_1 S(t) - \kappa + I_s(t)\rho - R(t)\vartheta - N(t)\nu + \lambda Q(t) + \theta I(t)\right) \\ &= \zeta(t)\left\{\left(U_{1,eq} - \frac{K}{S(t)} \operatorname{sgn}(\zeta(t))\right)S(t) - \kappa + I_s(t)\rho - R(t)\vartheta - N(t)\nu + \lambda Q(t) + \theta I(t)\right\} \\ &= \zeta(t)\left\{\left(\frac{1}{S(t)}\{\hat{\kappa} + R(t)\hat{\vartheta} + N(t)\hat{\nu} - I_s(t)\hat{\rho} - Q(t)\hat{\lambda} - I(t)\hat{\theta}\} - \frac{K}{S(t)} \operatorname{sgn}(\zeta(t))\right)S(t) - \kappa - I_s(t)\rho\right. \\ &\quad \left. - R(t)\vartheta - N(t)\nu + \lambda Q(t) + \theta I(t)\right\} \\ &= \zeta(t)\left\{(\hat{\kappa} - \kappa) + R(t)(\hat{\vartheta} - \vartheta) + N(t)(\hat{\nu} - \nu) - I_s(t)(\hat{\rho} - \rho)\right. \\ &\quad \left. - Q(t)(\hat{\lambda} - \lambda - I(t)(\hat{\theta} - \theta)) - K \operatorname{sgn}(\zeta(t))\right\} \\ &= \zeta(t)\left\{\hat{f} - f - K \operatorname{sgn}(\zeta(t))\right\}\end{aligned}$$

$$= \zeta(t)(\hat{f} - f) - K|\zeta(t)|. \quad (37)$$

According to assumption (35),

$$\begin{aligned} \frac{1}{2} \frac{d}{dt} \zeta(t)^2 &= \frac{1}{2} \frac{d}{dt} |\zeta(t)|^2 \\ &= \zeta(t)(\hat{f} - f) - K|\zeta(t)| \\ &\leq \zeta(t)F - (F + \eta)|\zeta(t)| \\ &\leq -\eta|\zeta(t)|. \end{aligned} \quad (38)$$

Note that Assumptions 1 and 2 have been used to prove that the time-derivative is always negative definite. Hence, $L(t)$ is positive definite, while $\dot{L}(t)$ is negative definite. Thus, according to Lyapunov's direct method, the equilibrium point at the origin $\zeta(t) = 0$ is globally asymptotically stable and, therefore, $L(t)$ tends to zero as time tends to infinity. All trajectories starting out the sliding surface $\zeta = 0$ must reach it in finite time and then will remain on this surface.

By integrating inequality (38) from 0 to t , we have

$$\zeta(t) - \zeta(0) \leq -\eta \int_0^t |\zeta(\tau)| d\tau. \quad (39)$$

So

$$\begin{aligned} \zeta(0) &\geq -\zeta(t) + \eta \int_0^t |\zeta(\tau)| d\tau \\ &\geq \int_0^t |\zeta(\tau)| d\tau \\ &\geq 0. \end{aligned} \quad (40)$$

If t on the unequal sides of (40) tends to infinity ($t \rightarrow \infty$), then

$$\lim_{t \rightarrow \infty} \int_0^t |\zeta(\tau)| d\tau \leq \zeta(0) < \infty. \quad (41)$$

That is, in this case, the above integral exists and is smaller and equal to $\zeta(0)$, since $\zeta(0)$ is positive and limited. According to Barbalat's Lemma, we have

$$\lim_{t \rightarrow \infty} \int_0^t |\zeta(\tau)| d\tau = 0. \quad (42)$$

Therefore, (42) shows reaching the sliding surface. Indeed in SMC, to have the property of invariance, reaching the sliding surface must occur in a limited time. According to (38),

$$\zeta \dot{\zeta} \leq -\eta|\zeta|. \quad (43)$$

Suppose that t_f is the time to reach the sliding surface, that is, $\zeta(t_f) = 0$. Now, consider the following two situations:

1. Suppose $\zeta > 0$. Therefore, using (43), we reach the following relationship:

$$\dot{\zeta} \leq -\eta. \quad (44)$$

By integrating the relation (44) between $t = 0$ and $t = t_f$, we have

$$-\zeta(0) \leq -\eta t_f. \quad (45)$$

So

$$t_f \leq \frac{\zeta(0)}{\eta}. \quad (46)$$

2. Suppose $\zeta < 0$. Therefore, using (43), we reach the following relationship:

$$\dot{\zeta} \geq \eta. \quad (47)$$

By integrating the relation (44) between $t = 0$ and $t = t_f$, we have

$$-\zeta(0) \geq \eta t_f. \quad (48)$$

So

$$t_f \leq \frac{-\zeta(0)}{\eta}. \quad (49)$$

Using relations (46) and (49), we have

$$t_f \leq \frac{|\zeta(0)|}{\eta}. \quad (50)$$

Therefore, for a finite time $t_f \leq \frac{|\zeta(0)|}{\eta}$, the sliding surface is reached. When this condition is met, the dynamic behavior of the tracking error (25) is given

$$\dot{e}(t) + \Gamma e(t) = 0. \quad (51)$$

Therefore, the control objective is achieved, and the defined tracking error tends to zero and total population tends to be Recovered. \square

According to assumption (33), the function F must be defined so that the appropriate switching gain can be obtained. For this reason, the switching gain is specified over time with adaptive control. Since system (2) contains parameters that are changing, then the online parameter estimation method is used in adaptive control. Also, in the numerical results section 4, gain switching in (35) has been obtained by the online estimation method. In this section, by using adaptive control, the switching gain is increased enough to reach the sliding level, and the sliding condition is established.

4 Numerical results

In this section, the performance of the proposed sliding mode controller is investigated on the system model (2), which has uncertainty parameters. The simulation of this model has been done using *MATLAB – R2021* software and system *Lenovo – B50*. The basic conditions for simulation are the relation (52),

$$(S(0), Q(0), I(0), I_s(0), R(0)) = (10000, 6000, 70, 3000, 30). \quad (52)$$

The parameter values of system (2) are given in Table 1.

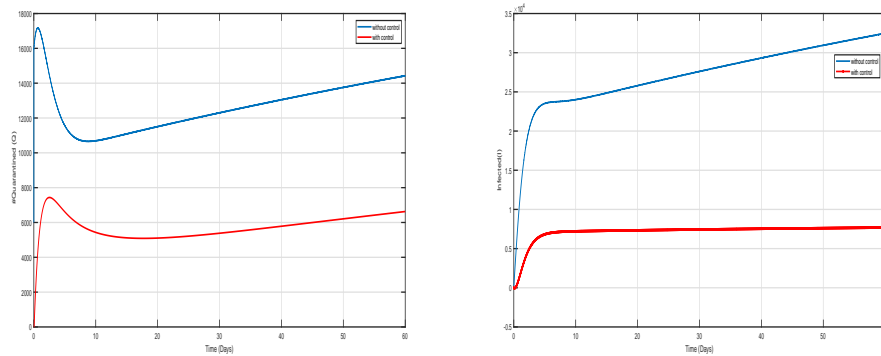


Figure 1: Left: quarantined people (Q). Right:infected people (I).

Table 1: The parameters of the model.

Parameter	Definition	Value
κ	Source rate of susceptible individuals	19100
β_0	Natural mortality rate	0.005
φ	Disease transmission rate	0.3
α	Quarantined rate	0.6
ε	Coronavirus (CoV) relapse rate	0.01
β	Infection rate	0.8
λ	Recovery rate of quarantined individuals	0.1
θ	Spontaneous recovery rate	0.7
δ	Isolation rate	0.1
σ	Cure rate from COVID 19	0.1
μ	Disease induced death rate	0.1

Figure 1 Left, shows the effects of educational campaign control u_1 and social distancing control u_2 on quarantined people for 60 days. In Figure 1 Left, it is obvious that the number of quarantined people will decrease with the application of controls. When there is no control on system (2), that is, $u_1 = u_2 = u_3 = 0$, the number of quarantined people first increases a little and then decreases; but on the 10th day onwards, the number of these people increases.

Figure 1 Right, shows the effect of control measures on infected people for 60 days. In this figure, it is clear that the number of infected people is increasing if the system is not controlled, but it shows a decreasing effect by applying control measures. Although the affected people have a very small decrease in the beginning and it increases again, it is probably because the effect of control u_2 and u_3 on these people is not high. Indeed, the number of infected people in [11], which is designed with optimal control, is always increasing; Figure 1 Right shows that the designed controls were able to have a greater impact on the number of these infected people.

Figure 2 Left, shows the effect of control measures u_1 , u_2 , and u_3 on the number of isolated people for 60 days. It can be seen here that these control measures significantly affect isolated people and reduce these people a lot,

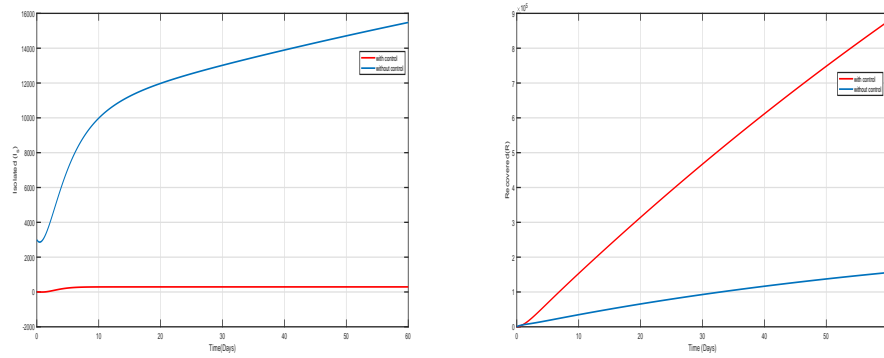


Figure 2: Left: isolated people (I_s). Right: recovered people (R).

so controls u_1, u_2 , and u_3 have had a good effect on these people. As can be seen, if there is no control, the number of isolated people is increased. According to the fact that in [11] the number of isolated people with optimal control has always been peaking and increasing, Figure 2 Left shows that the controllers proposed in this article have been able to reduce the number of these isolated people. Figure 2 Right, shows the effects of control measures such as educational campaign u_1 , social distancing u_2 , and treatment control u_3 . The number of recovered people for 60 days is observed in this case that the control measures had a great effect on the recovered people, so these controls were able to control the recovered people well. In the absence of control, the number of recoveries shows a small increase, which is less than expected and not appropriate.

Therefore, these control measures have been used to achieve the desired result, and the number of those people who have recovered increases rapidly. The number of these recovered people is [11] more than the simulated article.

Figure 3 shows the slight difference between the recovered population and the reference signal. As can be seen from the figure, the recovered population and the reference signal are superimposed, which means that the control objective is fulfilled. This difference can be eliminated by increasing the switching gain; in other words, with an increase of a in the suggested signal, the whole population is more inclined to be immune from this disease.

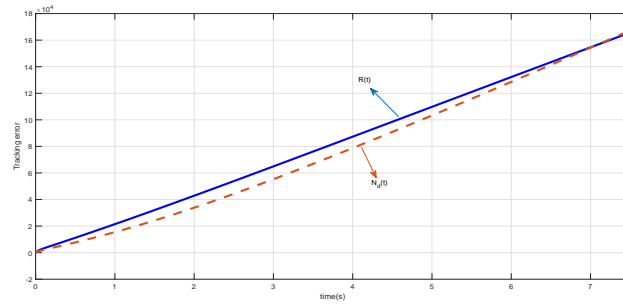


Figure 3: Tracking error.

Figure 4 shows the simulation of controls u_1 , u_2 , and u_3 separately, which also shows the stability of the controls.

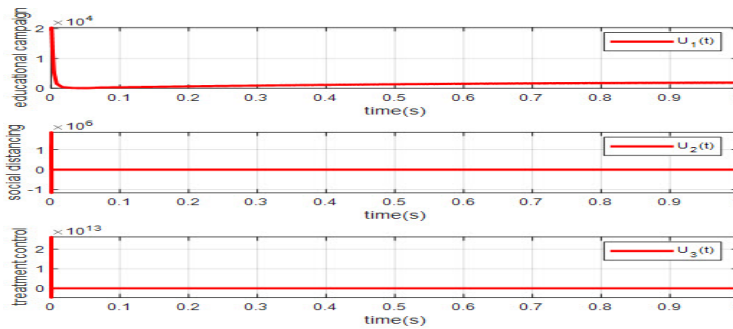


Figure 4: Controls u_1 , u_2 , and u_3 .

5 Conclusion

In this work, an epidemic model for the spread of the infectious disease COVID-19 in a population was studied. This model includes people who are susceptible, quarantined, infected, isolated, and removed. This model includes three controls: social distancing, educational campaign, and treatment control. Since this model has uncertainty parameters, it has been used after SMC to increase the removed individuals. In addition, because the parameters of the model have uncertainty, in the numerical simulation, the online parameters estimation method was used in the adaptive control for

appropriate gain switching. Finally, in order to evaluate the performance of the controllers and confirm the presented theoretical results, simulation has been done using MATLAB R2021a software. After checking the numerical results, it can be seen that the controllers of social distancing u_1 , educational campaign u_2 , and treatment control u_3 of the reduction of quarantined, infected, and isolated people are more effective; also, these controllers have a very good effect on the recovered people, and this shows that the controllers were able to prevent the spread of this disease to some extent. With regard to the discovery of the COVID-19 vaccine, as future research, by improving the aforementioned modeling and considering vaccinated people as an independent group and vaccination as another control strategy, the research can be developed.

References

- [1] Abdolkhaleghzade, S.M., Effati, S. and Rakhshan, S.A. *An efficient design for solving discrete optimal control problem with time-varying multi-delay*, Iranian Journal of Numerical Analysis and Optimization, 12(2) (2022), 719–738.
- [2] Bandyopadhyay, B., Deepak, F. and Kim, K-S. *Sliding mode control using novel sliding surfaces*, Springer. Berlin Heidelberg, Germany, 2009.
- [3] Barambones, O. and Alkorta, P. *A robust vector control for induction motor drives with an adaptive sliding-mode control law*, J. Frank. Inst. 348 (2) (2011), 300–314.
- [4] Barambones, O., Gonzalez de Durana, J. and de la Sen, M. *Robust speed control for a variable speed wind turbine*, Int. J. Innov. Comput. Inf. Control. 8 (11) (2012), 7627–7640.
- [5] Bartolini, G. and Pydynowski, P. *An improved, chattering free, V.S.C. scheme for uncertain dynamical systems*, IEEE Trans. Autom. Control. 41(8) (1996), 1220–1226.

- [6] Bartolini, G., Ferrara, A., Usai, E. and Utkin, V.I. *On multi-input chattering-free second-order sliding mode control*, IEEE Trans. Autom. Control. 45 (9) (2000), 1711–1717.
- [7] Bartolini, G., Pisano, A., Punta, E. and Usai, E. *A survey of applications of second-order sliding mode control to mechanical systems*, Int. J. Control. 76 (2003), 875–892.
- [8] Bhatnagar, V., Chandra Poonia, R., Nagar, P. and Kumar, S. *Descriptive analysis of COVID-19 patients in the context of India*, J. Interdiscip. Math. 24 (2020), 489–504.
- [9] Binti Hamzah, F.A., Lau, C., Nazri, H., Ligot, D.V., Lee, G., Tan, C.L. and et al. *Coronatracker: world-wide COVID-19 outbreak data analysis and prediction*, Bull. World Health Organ. 19 (32) (2020), 1–32.
- [10] Birkhoff, G. and Rota, G.C. *Ordinary differential equations*, 4th edition, JohnWiley & Sons, New York, 1989.
- [11] Biswas, M.H.A., Khatun, M.S., Paul, A.K., Khatun, M.R., Islam, M.A., Samad, S.A. and Ghosh, U. *Modeling the effective control strategy for the transmission dynamics of global pandemic COVID-19*, medRxiv, 2020.
- [12] Bogoch, I.I., Watts, A., Thomas-Bachli, A., Huber, C., Kraemer, M.U.G. and Khan, K. *Pneumonia of unknown aetiology in Wuhan, China: potential for international spread via commercial air travel*, J. Travel Med. 27(2) (2020), taaa008.
- [13] Brauer, F. and Castillo-Chavez, C. *Mathematical models in population biology and epidemiology*, 2, New York, Springer, 2012.
- [14] Cao, B. and Kang, T. *Nonlinear adaptive control of COVID-19 with media campaigns and treatment*, Biochem Biophys Res Commun. 555 (2021), 202–209.
- [15] Cao, S., Feng, P. and Shi, P. *Study on the epidemic development of COVID-19 in Hubei province by a modified SEIR model*, J. Zhe jiang Univ. Med. Sci. 49(2) (2020), 178–184.

- [16] Chung, Y.C., Wen, B.J. and Lin, Y.C. *Optimal fuzzy slidingmode control for biomicrofluidic manipulation*, Control Eng. Pract. 15(9) (2007), 1093–1105.
- [17] Clifford, S., Klepac, P., Zandvoort, K.V., Quilty, B., Eggo, R.M. and Flasche, S. *Interventions targeting air travellers early in the pandemic may delay local outbreaks of sars-cov-2*, medRxiv, 2020.
- [18] Comunian, A., Gaburro, R. and Giudici, M. *Inversion of an SIR-Based model: A critical analysis about the application to COVID-19 epidemic*, Physica D: Nonlinear Phenomena, 413 (2020), 132674.
- [19] Cooper, I., Mondal, A. and Antonopoulos, C.G. *A SIR Model Assumption for The Spread of COVID-19 in Different Communities*, Chaos. Solitons Fractals. 139 (2020), 110057.
- [20] Das, M. and Samanta, G.P. *A fractional order COVID-19 epidemic transmission model: Stability analysis and optimal control*, Comput. Math. Biophys. 9 (2021), 22–45.
- [21] Diekmann, O. and Heesterbeek, J.A.P. *Mathematical epidemiology of infectious diseases: model building, analysis and interpretation*, Wiley Series in Mathematical and Computational Biology, Chichester, Wiley, 2000.
- [22] Eubank, S., Eckstrand, I., Lewis, B., Venkatramanan, S., Marathe, M. and Barrett, C.L. *Commentary on Ferguson et al. Impact of non-pharmaceutical interventions (NPIs) to reduce COVID-19 mortality and healthcare demand*, Bull. Math. Biol. 82 (2020), 1–7.
- [23] He, S., Tang, S., Xiao, Y. and Cheke, R.A. *Stochastic modelling of air pollution impacts on respiratory infection risk*, B. Math. Biol. 80 (2018), 3127–3153.
- [24] Hengamian Asl, E., Saberi-Nadjafi, J. and Gachpazan, M. *2D-fractional Muntz–Legendre polynomials for solving the fractional partial differential equations*, Iranian Journal of Numerical Analysis and Optimization, 10(2) (2020), 1–31.

- [25] Ketabdari, A., Farahi, M. and Effati, S. *An approximate method based on Bernstein polynomials for solving fractional PDEs with proportional delays*, Iranian Journal of Numerical Analysis and Optimization, 10(2) (2020), 223–239.
- [26] Khan, M.K. and Spurgeon, S.K. *Robust MIMO water level control in interconnected twin-tanks using second order sliding mode control*, Control Eng. Pract. 14(4) (2006), 375–386.
- [27] Khanbehbin, T., Gachpazan, M., Effati, S. and Miri, S. *Shooting continuous Runge–Kutta method for delay optimal control problems*, Iranian Journal of Numerical Analysis and Optimization, 12(3) (2022), 680–703.
- [28] Koshkouei, A.J. and Zinober, A.S.I. *Robust frequency shaping sliding mode control*, IEE Proc. Control Theory Appl. 147 (2000), 312–320.
- [29] Lee, H. and Utkin, V.I. *Chattering suppression methods in sliding mode control systems*, Annu. Rev. Control. 31(2) (2007), 179–188.
- [30] Levant, A. *Sliding order and sliding accuracy in sliding mode control*, Int. J. Control, 58 (1993), 1247–1263.
- [31] Li, J., Xiao, Y., Zhang, F. and Yang, Y. *An algebraic approach to proving the global stability of a class of epidemic models*, Nonlinear Anal. Real World Appl. 13(5) (2012), 2006–2016.
- [32] Li, Y., Wang, B., Peng, R., Zhou, C., Zhan, Y., Liu, Z. and et al. *Mathematical modeling and epidemic prediction of COVID-19 and its significance to epidemic prevention and control measures*, Int. J. Curr. Res. 5(1) (2020), 19–36.
- [33] Mirhosseini-Alizamani, S.M. *Solving linear optimal control problems of the time-delayed systems by Adomian decomposition method*, Iranian Journal of Numerical Analysis of Optimization, 9(2) (2019), 165–185.
- [34] Mirhosseini-Alizamani, S.M., Effati, S. and Heydari, A. *An iterative method for suboptimal control of a class of nonlinear time-delayed systems*, Systems and Control Letters, 82 (2015), 40–50.

- [35] Mukandavire, Z., Malunguza, N., Cuadros, D., Shiri, T., Musuka, G. and Nyabadza, F. *Quantifying early COVID-19 outbreak transmission in south Africa and exploring vaccine efficacy scenarios*, SSRN Electronic Journal, 15(7) (2020), e0236003.
- [36] Murray, J.D. *Mathematical biology: An Introduction (interdisciplinary applied mathematics)*, New York, Springer, 2007.
- [37] Ngonghala, C.N., Iboi, E., Eikenberry, S., Scotch, M., MacIntyre, C.R., Bonds, M.H. and Gumel, A.B. *Mathematical assessment of the impact of non-pharmaceutical interventions on curtailing the 2019 novel coronavirus*, Math. Biosci. 325 (2020), 108364.
- [38] Perruquetti, W. and Pierre-Barbot, J., *Sliding mode control in engineering*, Marcel Dekker, 2002.
- [39] Prem, K., Liu, Y., Russell, T.W., Kucharski, A.J., Eggo, R.M., Davies, N., Flasche, S., Clifford, S., Pearson, C.A., Munday, J.D. and Abbott, S. *The effect of control strategies to reduce social mixing on outcomes of the COVID-19 epidemic in Wuhan, China: a modelling study*, The Lancet Public Health, 5(5) (2020), 261–270.
- [40] Saad-Roy, C.M., Wingreen, N.S., Levin, S.A. and Grenfell, B.T. *Dynamics in a simple evolutionary epidemiological model for the evolution of an initial asymptomatic infection stage*, Proc. Natl. Acad. Sci. USA, 117(21) (2020), 11541–11550.
- [41] Shu, H., Fan, D. and Wei, J. *Global stability of multi-group SEIR epidemic models with distributed delays and nonlinear transmission*, Non-linear Anal. Real World Appl. 13(4) (2012), 1581–1592.
- [42] Silverman, J.D., Hupert, N. and Washburne, A.D. *Using influenza surveillance networks to estimate state-specific prevalence of SARS-CoV-2 in the United States*, Sci Transl. Med. 12(554) (2020), eabc1126.
- [43] Singh, V., Poonia, R.C., Kumar, S., Dass, P., Agarwal, P., Bhatnagar, V. and Raja, L. *Prediction of COVID-19 corona virus pandemic based on time series data using Support Vector Machine*, J. Discrete Math. Sci. Cryptogr. 23(8) (2020), 1583–1597.

- [44] Su, J.-P. and Wang, C.-C. *Complementary sliding control of non-linear systems*, Int. J. Control, 75(5) (2002), 360–368.
- [45] Tang, B., Bragazzi, N.L., Li, Q., Tang, S., Xiao, Y. and Wu, J. *An updated estimation of the risk of transmission of the novel coronavirus(2019-ncov)*, Infect. Dis. Model. 5 (2020), 248–255.
- [46] Tang, B., Wang, X., Li, Q., Bragazzi, N.L., Tang, S., Xiao, Y. and Wu, J. *Estimation of the transmission risk of the 2019-ncov and its implication for public health interventions*, J. Clin. Med. 9(2) (2020), 462.
- [47] Verity, R., Okell, L.C., Dorigatti, I. and et al. *Estimates of the severity of coronavirus disease 2019: A model-based analysis*, Lancet Infect Dis. 20(6) (2020), 669–677.
- [48] Wu, J.T., Leung, K. and Leung, G.M. *Nowcasting and forecasting the potential domestic and international spread of the 2019 nCoV outbreak originating in Wuhan, China: a modeling study*, The Lancet. 395(10225) (2020), 689–697.
- [49] Xiong, H. and Yan, H. *Simulating the infected population and spread trend of 2019-ncov under different policy by EIR model*, Available at SSRN 3537083, 2020.
- [50] Yang, C., Yang, Z., Huang, X., Li, S. and Zhang, Q. *Modeling and robust trajectory tracking control for a novel six-rotor unmanned aerial vehicle*, Math. Probl. Eng. 2013(1) (2013), 673525.
- [51] Young, K.D. and Özgüner, U. *Frequency shaping compensator design for sliding mode*, Int. J. Control, 57 (1993), 1005–1019.
- [52] Zhang, M., Wang, X. and Cui, J. *Sliding mode of compulsory treatment in infectious disease controlling*, Math. Biosci. Eng. 16(4) (2019), 254–2561.
- [53] Zhang, X.Y., Zhao, Y.X., Xin, D.X. and He, K.P. *Sliding mode control for mass moment aerospace vehicles using dynamic inversion approach*, Math. Probl. Eng. 2013(1) (2013), 284869.

- [54] Zhou, X. and Cui, J. *Analysis of stability and bifurcation for and SEIR epidemic model with saturated recovery rate*, Commun. Nonlinear Sci. Numer. Simul. 16(11) (2011), 4438–4450.
- [55] Zhou, W., Xiao, Y. and Heffernan, J.M. *A two-thresholds policy to interrupt transmission of West Nile Virus to birds*, J. Theor. Biol. 463 (2019), 22–46.